Tribology Letters (2020) 68:38
https://doi.org/10.1007/s11249-020-1279-z

ORIGINAL PAPER

A Comparison of Airborne Particles Generated from Disk Brake Contacts: Induction Versus Frictional Heating

Jijie Ma[1,2] · Ulf Olofsson[1] · Yezhe Lyu[1] · Jens Wahlström[1] · Anna Hedlund Åström[1] · Minghui Tu[1]

Received: 11 December 2019 / Accepted: 29 January 2020 / Published online: 12 February 2020

Abstract

Volatile emissions of vehicle brakes relate to the high temperature of the brake friction pair. However, as a passive parameter of braking applications, temperature is usually studied together with other parameters such as sliding speed and load. Heating tests that increase the friction pair temperature with an induction heater instead of friction are proposed in this study to imitate the rise in temperature in friction tests. Non-friction airborne particles produced solely by the high temperature in heating tests were studied in comparison with friction tests. The results confirmed the existence of non-friction airborne particles and they can represent about 4.5% of the total airborne particles in friction tests. The high-temperature behaviour as well as the composition of the non-friction airborne particles is also presented.

Graphical Abstract

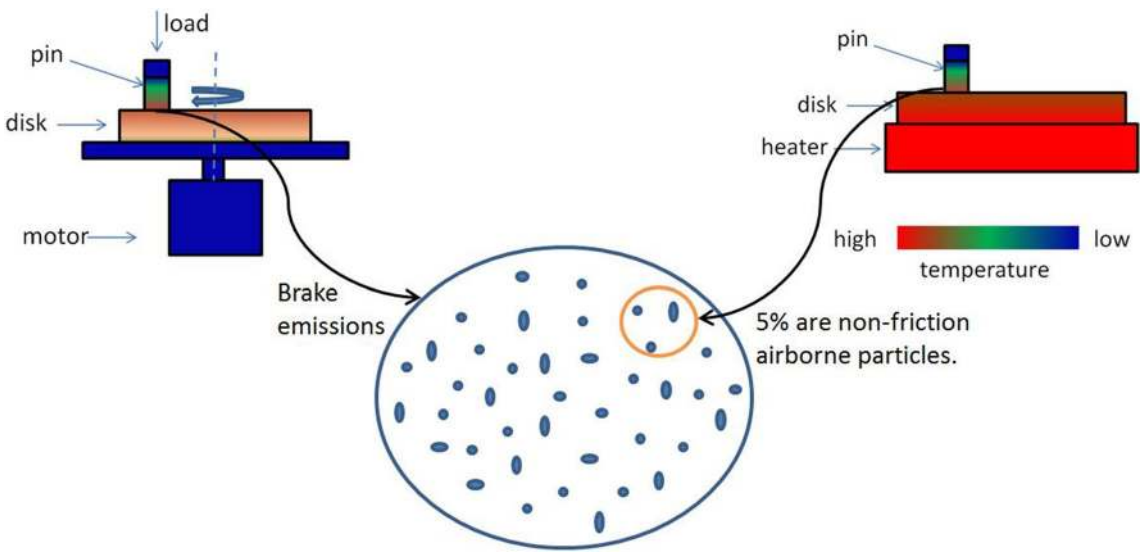

Keywords Brake airborne particles · Volatiles · Temperature

1 Introduction

Airborne particles from road vehicles emissions can have adverse effects on human health [1, 2]. A significant portion of these emissions come from non-exhaust processes, such as brake, tyre, road wear, and road dust resuspension [3]. Since exhaust emissions have been successfully reduced by

✉ Ulf Olofsson
ulfo@md.kth.se

[1] Department of Machine Design, Industrial Engineering and Management, KTH Royal Institute of Technology, 100 44, Stockholm, Sweden

[2] College of Engineering, Zhejiang Normal University, Jinhua, China

Table 1 The critical temperature of brake emission

Authors	Critical temperature	Pad Material	Testing machine
Wahlström et al. [6]	Around 200 °C pin	LM	Pin-on-disk
Wahlström et al. [7]	Around 200 °C disk	LM	Pin-on-disk
Alemani et al. [8]	170–190 °C disk	LM	Pin-on-disk
Nosko et al. [20]	120 °C disk	LM & NAO	Pin-on-disk
Zum Hagen et al. [9]	140–170 °C disk	LM	Dyno
Kukutschová et al. [21]	Around 300 °C disk	LM	Dyno
Perricone et al. [11]	Around 200 °C disk	LM	Dyno
Mathissen et al. [10]	160 °C disk	LM	Dyno & Road

LM low-metallic, *NAO* non-asbestos organic, *Dyno* dynamometer

means of regulation, non-exhaust emissions will become the dominant urban source of particulate matter, especially with the broadening use of new energy vehicles like fuel cell, electric or hybrid vehicles. Particulate matter, from the perspective of diameters, can be classified into coarse (> 2.5 μm in aerodynamic diameter), fine (0.1–2.5 μm) and ultrafine (< 0.1 μm), or PM_{10} (mass of particles in $\mu g/m^3$ with aerodynamic diameter less than 10 μm), $PM_{2.5}$ (less than 2.5 μm) and $PM_{0.1}$ (less than 0.1 μm) [4]. Timmers et al. [5] state that non-exhaust sources will account for more than 90% of PM10 and 85% of PM2.5 emissions from passenger cars, and the proportion is likely to increase as vehicles become heavier.

As a major source of non-exhaust emissions, brake particulate matter depends on the characteristics of the friction pair and brake parameters like speed, load and temperature. Wahlström et al. [6, 7] studied the airborne particles with a pin-on-disk machine working at different loads. The concentration of ultrafine/fine particles increased dramatically at the highest load levels. Alemani et al. [8] observed the particle concentration regarding friction power as the combination of the rotor speed and load. Zum Hagen et al. [9] confirmed in a dynamometer test that ultrafine particles occurred at temperatures between 140 and 170 °C. The importance of temperature, especially the critical temperature, was also confirmed by Mathissen et al. [10] in a road test. The detailed critical temperature and corresponding test machines are listed in Table 1.

The number of particles and the volume concentration in the ultrafine range is several magnitudes greater above the critical temperature as compared to below. Perricone et al. [11] found that volatiles were generated on the most severe test cycle where the temperature was above the critical temperature. It is also demonstrated in this paper that the concentration of brake aerosols decreased by several magnitudes after being heated by a sampling line at 200 °C. Plachá et al. [12] further studied the volatile organic compounds of brake airborne particles and confirmed the existence of BTEX (benzene, toluene, ethylbenzene and xylenes) and PAHs (polycyclic aromatic hydrocarbons) groups. Nosko et al. [13] studied the volume fraction of ultrafine airborne particles over temperature and found that the volume fraction above the critical temperature increased sharply to tens of percents.

Although the critical temperature for brake airborne particle emission is found, the direct influence of temperature on airborne brake emissions is still unknown. Unlike speed and load, temperature is a passive parameter affected by all brake conditions [8], which means that any modification in brake parameters will lead to a change in temperature. In order to decouple temperature into an independent parameter, a new way to simulate the temperature change in friction

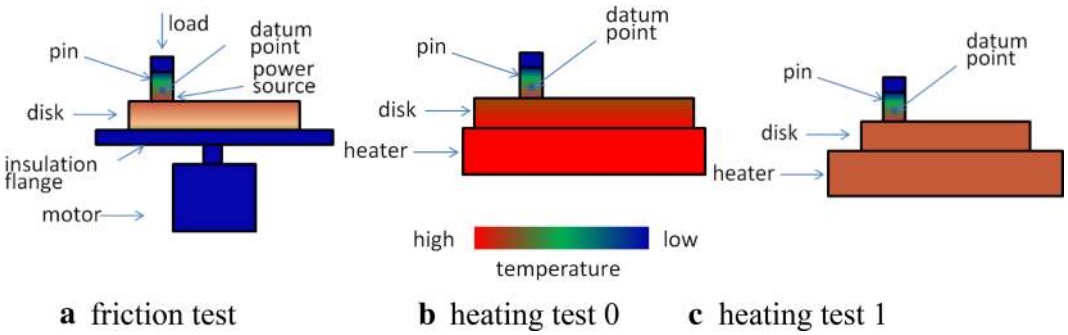

Fig. 1 Temperature distribution of the friction test and the heating test

tests is required. This study proposes a heating test using a heater for temperature control to find out if airborne particles (non-friction) can be generated by heating the friction pair without sliding.

2 Methodology

2.1 Method

The friction test in this study was conducted on a pin-on-disk machine. The normal pressure of the pin was loaded in the vertical direction and the disk rotated, driven by a servo motor. The friction power from the contact surface warms up both the pin and disk, leading to the rise in temperature in friction tests. In order to imitate the rise in temperature in the friction test, the heating test should transfer energy to both the pin and the disk. Generally, there are three ways to heat the friction pair: from the ambient air, from the pin and from the disk. Heating from the ambient air changes the air temperature, which would be different from friction tests and might have an impact on the airborne particles. Since brake friction materials of the pin are usually not as thermally conductive as the cast iron disk, mainly to avoid a rise in temperature of the brake fluid [14], heating from the disk is the best choice for heating tests.

The friction test and the heating test have different power sources to warm up the friction pair: the friction test at the contact surface and the heating test from the lower surface of the disk. As a result, the temperature distributions of the two tests are different, as shown in Fig. 1a, b. The temperature of the friction pair in the friction test [15] reaches its peak at the contact surface and decreases as it is farther away. The heating test temperature decreases in the order of the heater, the disk, and the pin. Thus, the two tests have different temperature distributions. Given the following hypotheses, the temperature of the two tests would be more comparable: (1) pins come from the same batch and have the same properties; (2) the disk has good thermal conductivity; (3) the radius and thickness of the disk is comparatively small. Hypothesis (1) ensures that temperatures of the pins in both tests will be completely matched. Hypothesis (2) and (3) would make the disk temperature evenly distributed, as shown in Fig. 1c. This means smaller disks are preferable in test design. A datum point on the pin, 2.5 mm above the contact surface as marked in Fig. 1, was selected since pins are relatively stationary in both tests while the disk rotates in the friction test.

2.2 Test Setup

2.2.1 Specimens

Specimens of disks and pins for both the friction and heating test were machined from the same batch of brake rotors and Cu free pads for a commercial passenger car in use in Europe. The disk was made of cast iron, 58 mm in diameter and 6 mm in thickness. The cylindrical pin was 10 mm in diameter and 17 mm in height.

2.2.2 Test Machine Setup

Test machines for both the friction test and the heating test were based on a one-way ventilated chamber for airborne

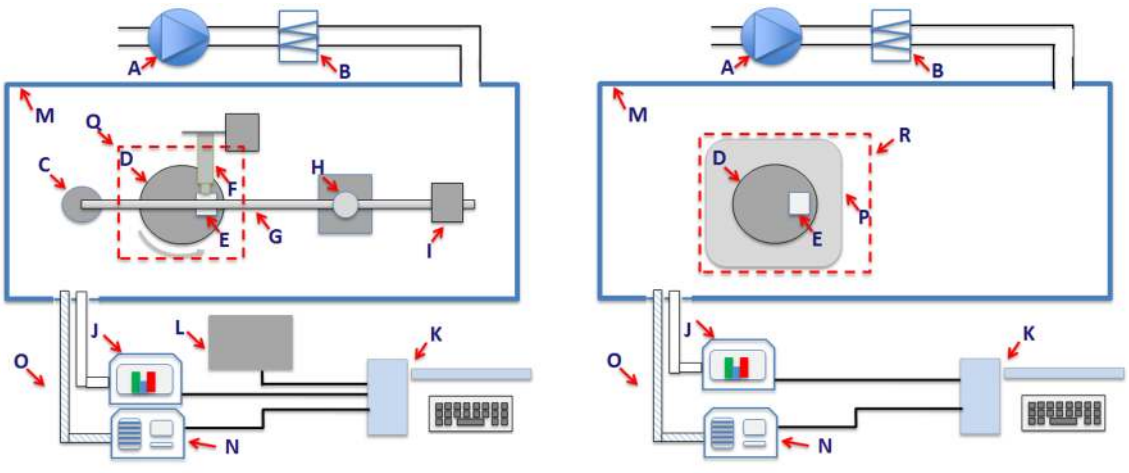

Fig. 2 A-pump, B-filter, C-loading weight, D-disk, E-pin, F-friction sensor, G-loading beam, H-universal bearing, I-counterweight, J-FMPS, K-industrial computer, L-control cabinet of the tribometer, M-chamber, N-ELPI+, O-sampling line, P-heater, Q- friction assembly in Fig. 1a, R-heating assembly in Fig. 1c

Table 2 Design of comparison tests

No	Type	Sampling line temperature (°C)	Duration (H)	Test tag
1	Friction	23	2	Fric23 (Fric23_1, Fric23_2)
2	Friction	180	2	Fric180 (Fric180_1, Fric180_2)
3	Heating	23	2	Heat23 (Heat23_1, Heat23_2)
4	Heating	180	2	Heat180 (Heat180_1, Heat180_2)

emissions: a flow-adjustable clean air source, a sealed chamber for test facilities, instruments for counting and collecting airborne particles. A heated sampling line between the outlet of the chamber and the instrument is utilized to study the high-temperature effect (volatility) of the airborne particles. The composition of airborne particles could be detected with SEM (Scanning Electron Microscope) and EDS (Energy Dispersive X-ray Spectroscopy) [16]. The morphology of these particles could be observed with both SEM and light optical microscope (LOM, hereafter).

The friction test setup, shown in Fig. 2a, was proposed by Olofsson et al. [17]. The pin-on-disk tribometer (C, D, E, F, G, H, I in Fig. 2a) was placed in the one-way ventilated chamber. The heating test setup, shown in Fig. 2b, replaced the pin-on-disk tribometer with a heating unit while keeping the airborne emission assembly (A, B, J, K, L, M, N, O in Fig. 2a) the same. Airborne particles were counted and collected with ELPI + (Electrical Low Pressure Impactor) and FMPS (Fast Mobility Particle Sizer) with detecting ranges of 6–9840 nm and 6–560 nm, respectively. The ELPI + measures particles in an aerodynamic diameter and the FMPS measures particles in a mobility diameter. Two versions of the ELPI + instrument were used. One was a standard ELPI + and the other was a high-temperature version including a heated sampling line (O in Fig. 2) as well as heated particle collecting plates.

2.2.3 Test Design

A group of comparison tests were designed with the aim of finding temperature-originated non-friction airborne particles and their high-temperature behaviour (volatility). The existence of non-friction airborne particles was studied by comparing the heating and friction tests. The high-temperature behaviour was studied with the high-temperature version of the ELPI + instrument set at 180 °C (the same as [11]). Each test was repeated twice. The final test design is shown in Table 2.

It was also necessary to find appropriate test parameters with pre-tests so that temperatures of the heating test and the friction test could match well. Pre-tests for both friction and heating tests were conducted: friction pre-tests were to confirm brake conditions that can cover the critical temperature, heating pre-tests were to find the heating parameters that can produce a similar rise in temperature to that of the friction test. Before the heating test commenced, the heater was run on its own for a long period to clean the background airborne particles, until the measured particle number concentration in FMPS was zero.

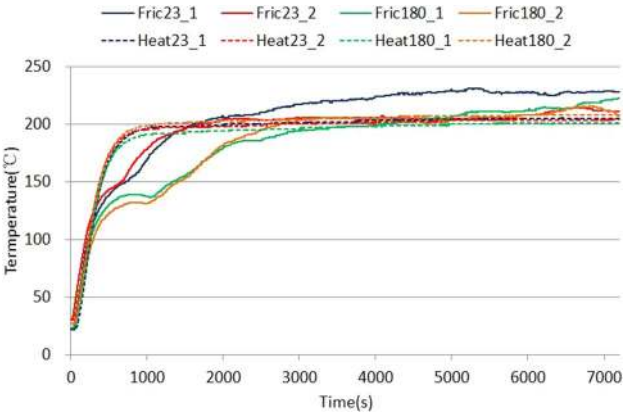

Fig. 3 Pin temperatures as measured in the pre-tests

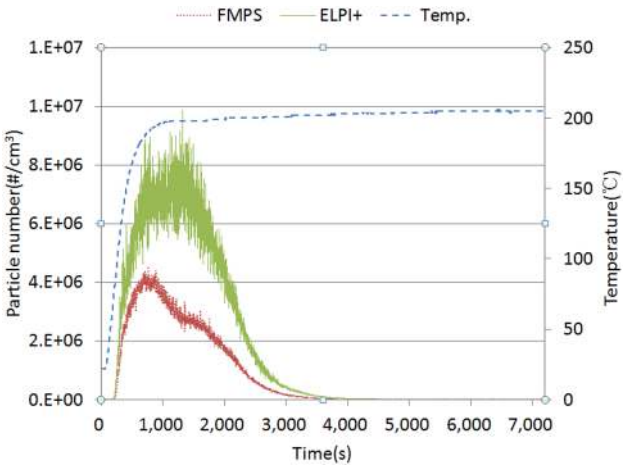

Fig. 4 Particle number history of Heat23_1

3 Test Results

3.1 Pre-test Results

Pre-tests were designed to find appropriate test parameters for both friction and heating tests. In friction pre-tests, a series of load and speed combinations were tested with the load from 2 to 4 kg and the speed from 900 to 1700 rpm. The final steady state temperature was selected to be around 200 °C at 3 kg and 1300 rpm, corresponding to 0.8 MPa and 3.3 m/s, which covered the critical temperature by producing particle number concentration at 10^8 #/cm^3 level. Heating pre-tests were to produce the same steady state temperature with an induction heater. The pin temperature was measured with an independent infrared thermometer (LS-MA-D2006-01-A by Optris Gmbh, Germany), the same instrument as in the friction tests. The appropriate set value of the heater was found by increasing it step by step and observing the pin temperature. The final steady state pin temperature was also around 200 °C, very close to the friction pre-tests.

Figure 3 illustrates the temperature data of the comparison tests. The temperatures of friction tests were not as steady as heating tests since they had impact on the friction coefficient which in turn affected the rise in temperature. The average temperatures of the friction and heating tests after two hours duration were 192 °C and 193 °C, respectively.

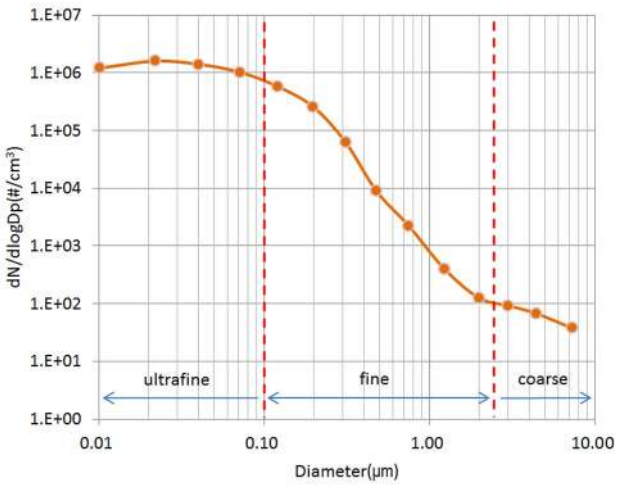

Fig. 5 Size distribution of Heat23_1

3.2 Airborne Particles Directly Originated from Temperature

Heat23 was the heating test aiming to see if airborne particles directly originated from temperature (also named non-friction airborne particles) exist. With the background being cleaned in the preparation test, all airborne particles,

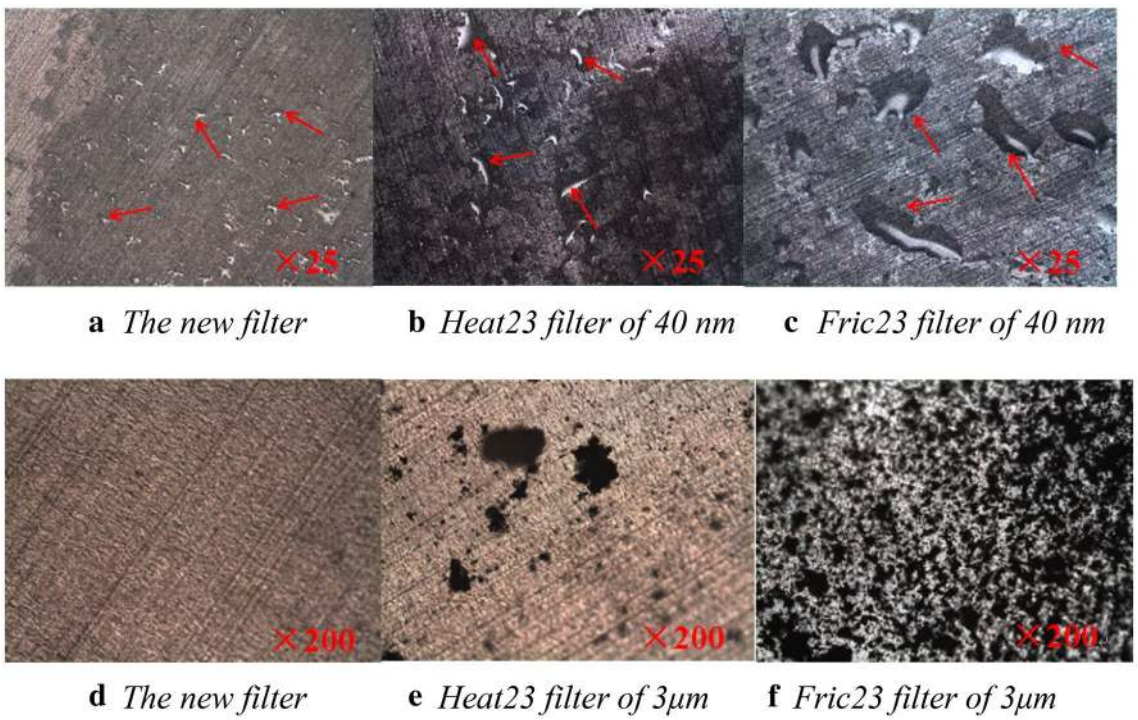

Fig. 6 LOM comparison of heating and friction tests versus the background for particles collected with an aerodynamic mean diameter of 40 nm and 3 μm, respectively

if observed, would originate from the friction pair. Figure 4 demonstrates the airborne particles of test Heat23_1 recorded by ELPI + and FMPS. The airborne particle concentration increased dramatically to the level of 10^6 #/cm^3 and decreased to almost zero about an hour later, which means a large amount of airborne particles were produced by heating the friction pair. A similar trend happened in the repeated test as well. Figure 5 further illustrates the size distribution of the same test as measured with the ELPI + instrument, which shows that ultrafine particles dominate the particle number.

The airborne particles were also collected on ELPI + greased Aluminium filters and observed with an LOM, as shown in Fig. 6. A new filter, used as the reference, was also observed at the same magnification. Droplets (indicated by arrows in Fig. 6) could be found in the filters from size channel 4 (40 nm in mean aerodynamic diameter) in both heating and friction tests. Similar droplets could also be identified on the new untested filter. But the sizes of the droplets were obviously different: small, medium and big droplets were found on the untested, the heating test and the friction test, respectively. This means additional particles were added to the filters and combined into larger droplets. The heating tests seem to produce fewer ultrafine particles than friction tests since the droplets were smaller in heating tests. In the coarse particle channel (Fig. 6d–f), the same trend as the ultrafine channel (Fig. 6a–c), was observed, as the particle number of the new filter, the heating test and the friction test increased in turn.

3.3 The Fraction of Non-friction Airborne Particles

It has been shown in Sect. 3.2 that the high temperature of the friction pair can produce non-friction airborne particles. Since temperature is a common parameter of both the heating and friction test, it can be inferred that non-friction airborne particles also exist in high-temperature friction tests. The fraction of non-friction airborne particles in friction tests can be calculated by comparing the heating test with the friction test. Figure 7 illustrates the airborne particle distribution as measured by ELPI + and FMPS, respectively. ELPI + and FMPS data show a similar trend of size distribution of airborne particle numbers. An intersection can be seen at the diameter of around 0.2 µm where heating tests produce less airborne particles to the left and more to the right as compared with friction tests.

The fraction of non-friction airborne particles to friction tests ($f_{\text{non-friction}}$) is calculated with the average particle number concentration (APNC) of the two tests. As some channels of FMPS were over-range in friction tests, the fraction was calculated with the data from ELPI + . The APNC of ELPI + in Eq. 1 is the average of PN10 (particle number concentration with aerodynamic diameter less than 10 um) over a duration of two hours. Non-friction airborne particles contribute about 5% to the total particle number of friction tests according to Eq. 1.

$$f_{\text{non}-\text{friction}} = \frac{APNC(Heat23\_1) + APNC(Heat23\_2)}{APNC(Fric23\_1) + APNC(Fric23\_2)} \quad (1)$$

The contribution of ultrafine particles is also calculated in terms of volume ($fV_{ultrafine}$) and number ($fN_{ultrafine}$) fractions that are the quotients of ultrafine particles and the total ones, as shown in Eq. 2 and Eq. 3.

$$fV_{ultrafine} = \frac{V_{ultrafine}}{V_{total}} = \frac{\sum_{Dp_i=0.006\mu m}^{0.1\mu m} V_{Dp_i}}{\sum_{Dp_i=0.006\mu m}^{10\mu m} V_{Dp_i}} \quad (2)$$

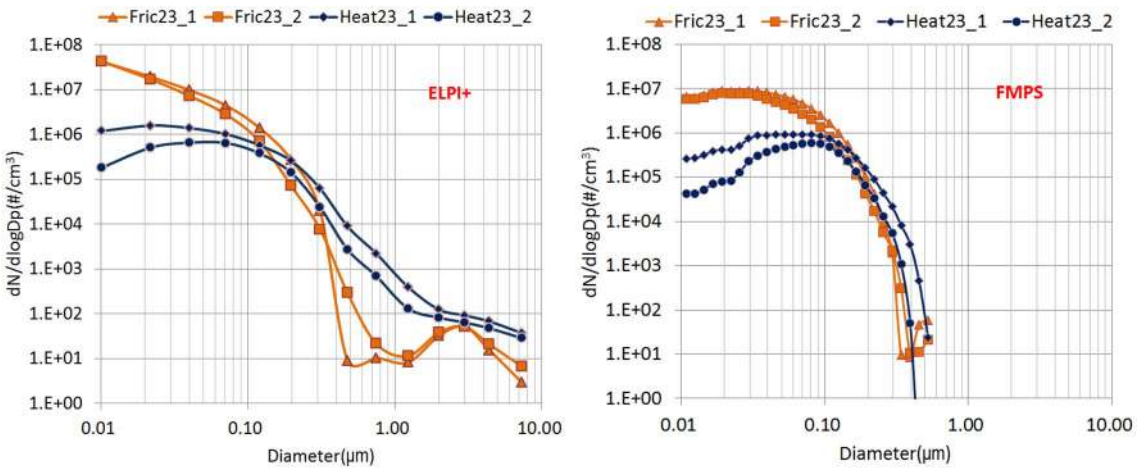

Fig. 7 Mean size distribution of heating and friction tests

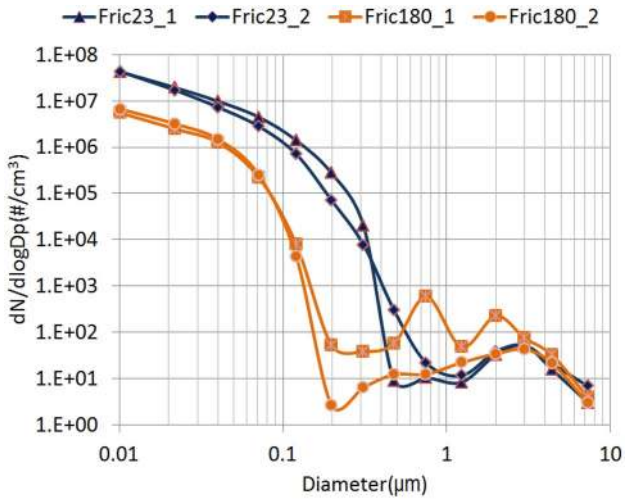

Fig. 8 Mean size distribution of friction tests

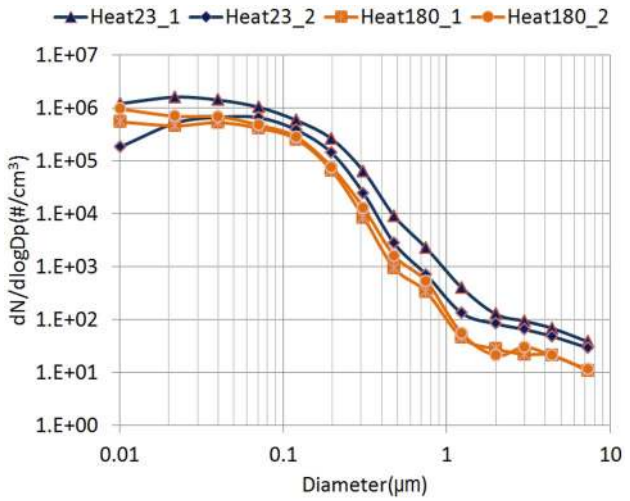

Fig. 9 Mean size distribution of heating tests

$$fN_{ultrafine} = \frac{PN_{ultrafine}}{PN_{total}} = \frac{\sum_{Dp_i=0.006\mu m}^{0.1\mu m} PN_{Dp_i}}{\sum_{Dp_i=0.006\mu m}^{10\mu m} PN_{Dp_i}} \quad (3)$$

In friction tests, the average volume fraction of ultrafine particles is 19%, like [13] that were about 7–21% at around 200 °C. The average volume fraction of ultrafine particles is only 1% in heating tests, much lower than friction tests. Ultrafine particles dominate the particle number in both heating and friction tests by fractions of 82% and 98%, respectively.

3.4 The Effect of High Temperature of Sampling and Collection on Non-friction Airborne Particles

High-temperature behaviour was studied with the high-temperature version of the ELPI + instrument whose temperature was controllable. FMPS was not included in this section since it used a regular sampling tube without a heating function, as shown in Fig. 2. Figure 8 shows the mean size distribution of airborne particles at 180 and 23 °C in friction tests. The high temperature of the heated sampling line removes a large number of airborne particles with a diameter of less than 300 nm. But the coarse particles are almost unchanged. Figure 9 demonstrates the size distribution of airborne particles in heating tests. A small part of airborne particles are removed in channels below 1 μm. The removed part increases in channels above 1 μm as the gap between Heat23 and Heat180 widens.

The detailed fractions (f_{heat} and $f_{friction}$) of airborne particles measured by the high-temperature version of the ELPI + are calculated. 33% of airborne particles are removed in heating tests according to Eq. 4 while the number is 86% in friction tests according to Eq. 5.

$$f_{heat} = 1 - \frac{APNC(Heat180\_1) + APNC(Heat180\_2)}{APNC(Heat23\_1) + APNC(Heat23\_2)} \quad (4)$$

$$f_{friction} = 1 - \frac{APNC(Fric180\_1) + APNC(Fric180\_2)}{APNC(Fric23\_1) + APNC(Fric23\_2)} \quad (5)$$

3.5 Composition of Non-friction Airborne Particles

It is already shown in Fig. 6 that both ultrafine and coarse particles can be found on the filters of heating tests. This section will further study the composition of these non-friction airborne particles. Although non-friction airborne particles cover the whole 6–9840 nm range, fine particles will not be included in this composition analysis since collections of fine channels contain only droplets which have a similar size to the new filter.

3.5.1 Ultrafine Particles

Composition of the ultrafine particles was studied with SEM Energy dispersive X-ray Spectroscopy. Figures 10 and 11 demonstrate the Back-Scattered Electron (BSE) pictures and compositions of size channel 4 of both tests. By comparing the SEM and LOM pictures, it can be inferred that the dark spots in the SEM are the droplets in the LOM. Further EDS analysis, shown in Figs. 10 and 11, confirms similar compositions of both tests. The backgrounds, area 1 of both tests, are mainly Aluminium accompanied with some Carbon and a little Oxygen, Iron, etc. Aluminium comes from the foil of

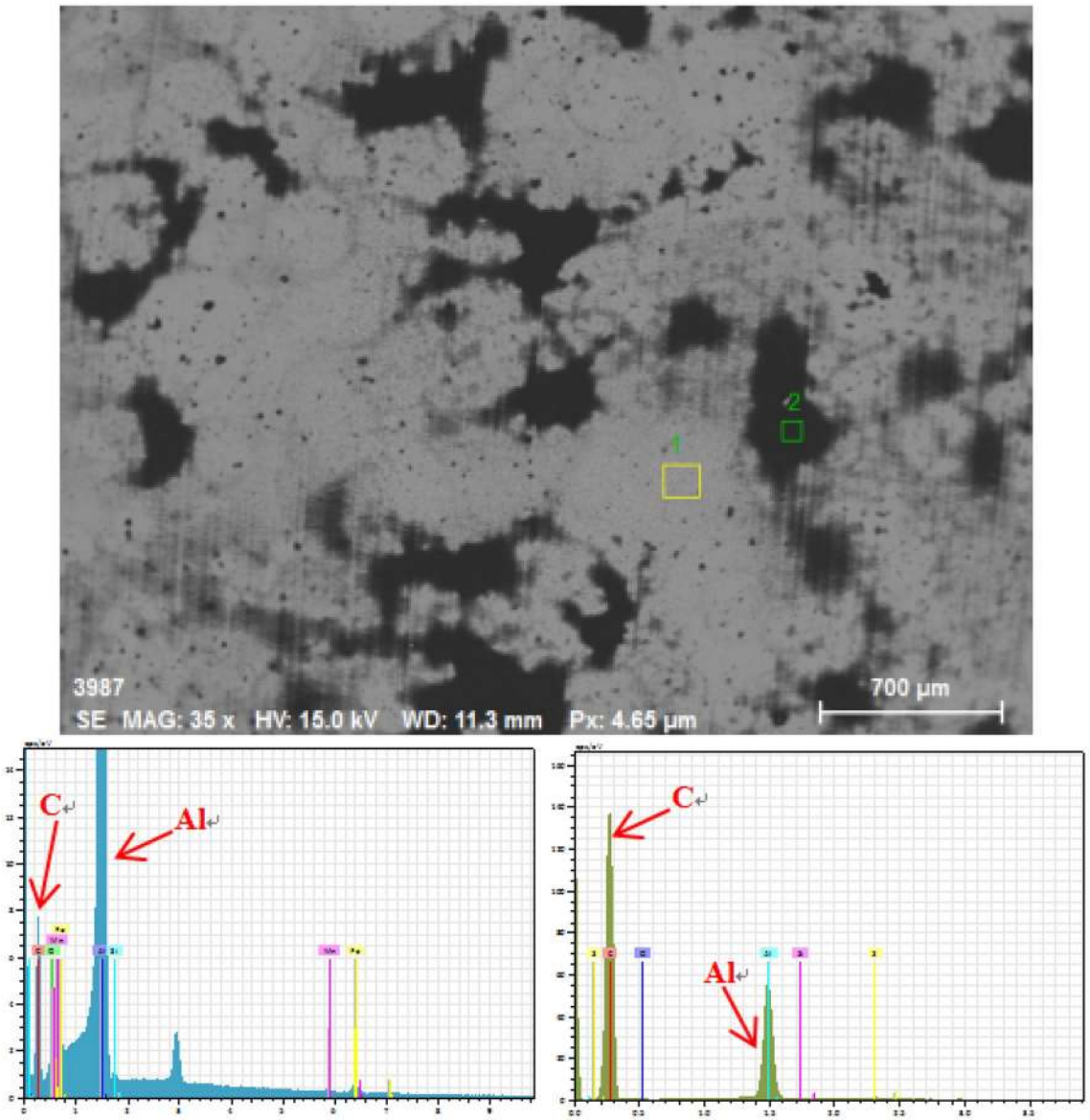

Fig. 10 Particles collected in the 40 nm channel of Heat23. Upper: SE image with the EDX areas marked. Lower left: Elements area 1. Lower right: Elements area 2

the filter and Carbon from the grease of the filter. Carbon in the background area is much lower than Aluminium. Compositions of the dark spots in both tests are mainly Carbon and Aluminium accompanied with a little Oxygen, Sulphur, etc. In both the friction and heating tests, the value of Carbon is larger than Aluminium in area 2 (dark spots), different to the background filter levels. This means the dark spots are accumulated organic compounds. According to the European Union Publications Office [18], a VOC is any organic compound having an initial boiling point less than or equal to 250 °C measured at a standard atmospheric pressure of 101.3 kPa. The ultrafine particles generated in heating tests could be identified as volatiles, as they are airborne organic compounds heated to a temperature around 200 °C. Figure 11a shows more dark area (organic compounds) than Fig. 10a, which implies that friction tests produce more ultrafine volatiles than heating tests.

3.5.2 Coarse Particles

Coarse particles were found in the coarse channels of both heating and friction tests. SEM–EDS mapping were conducted to compare the coarse particle composition in both tests. Comparing Figs. 12b and 13b, coarse particles from friction tests seem to involve more elements than those from heating tests. However, the dominant elements are quite

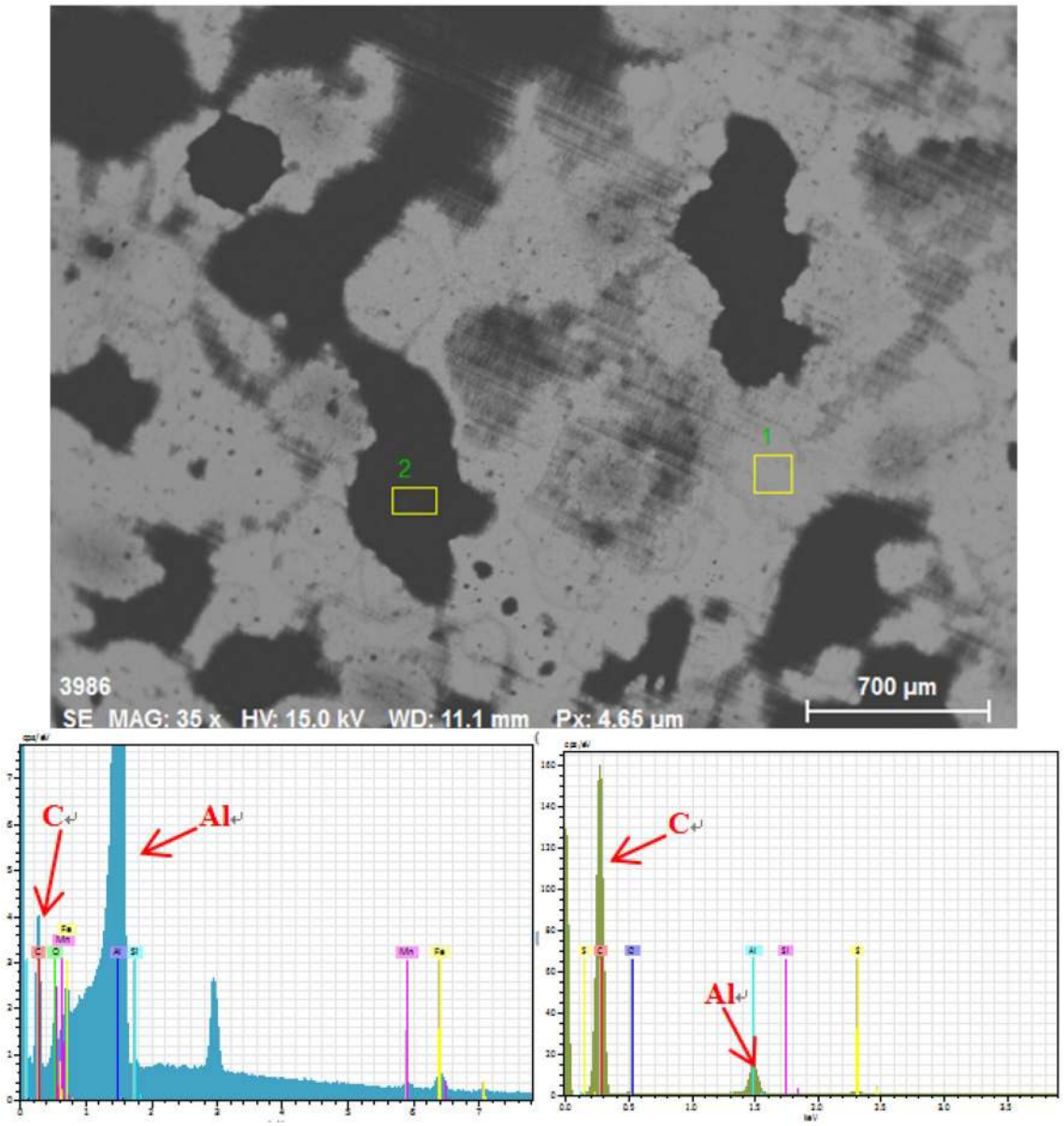

Fig. 11 Particles collected in the 40 nm channel of Fric23. Upper: SE image with the EDX areas marked. Lower left: Elements area 1. Lower right: Elements area 2

similar, including Aluminium, Carbon, Oxygen, Silicon and Iron. Taking a further observation of Oxygen, Figs. 12d and 13d, the coarse particles in both tests seem to be Oxides as Oxygen has almost the same distribution as coarse particles.

4 Discussion

4.1 Volatiles

It has been discussed by Perricone [11] and Plachá [12] that volatiles play a significant role in brake airborne emissions. Section 3.5.1 confirmed the existence of volatiles again from the perspective of composition. However, only channel 4, where the most obvious large droplets were found, was discussed in Sect. 3.5.1. It is usually volatiles in brake airborne emissions that are removed by external heating instruments, like the thermodenuder or the high-temperature version of ELPI + in [11]. Since airborne particles in heating tests were reduced in almost all channels (except the finest one) with the high-temperature version of ELPI + on, as shown in Fig. 9, an inference could be made that heating tests generate volatiles with diameters from 20 nm to 10 µm.

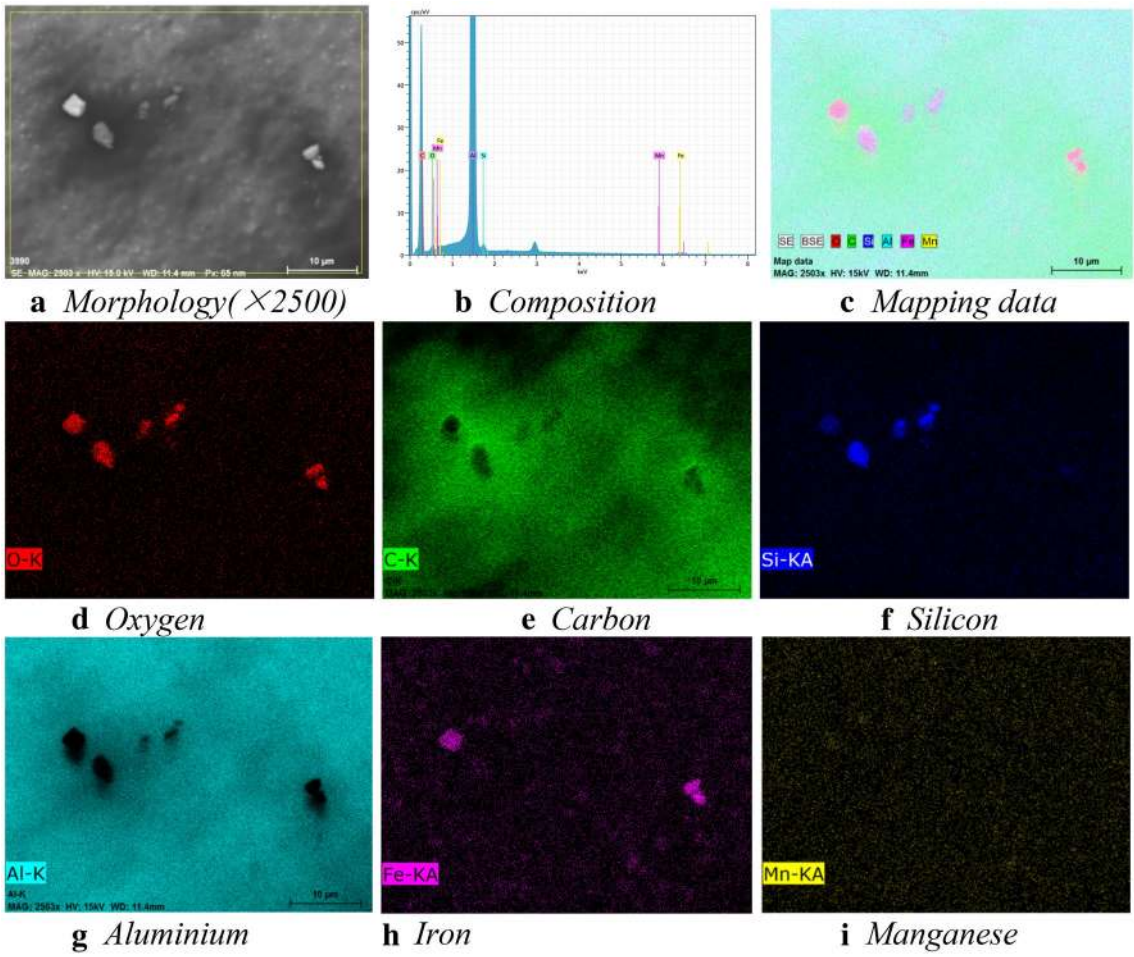

Fig. 12 Energy mapping of particles in channel 13 of Heat23

Figure 7 shows an intersection that there are more airborne particles with diameters above 0.2 µm in heating tests than in friction tests. Friction tests generate friction and non-friction airborne particles, while heating tests generate non-friction airborne particles. Non-friction airborne particles in the friction and heating tests should be approximately equal, since the two tests have a similar temperature of the friction pair. This means friction tests should have more airborne particles, which contradicts to the intersection in Fig. 7. A possible reason for this paradox might be related to the difference in ingredients. For heating tests, volatiles exist in almost all channels, with coarse channels mixed with a small amount of solid particles. For Friction tests, fine and coarse channels are dominated by friction debris and ultrafine channels have more volatiles. The turning point of friction debris and volatiles in friction tests is also around 0.2 µm according to LOM pictures at the 50 times magnification in Fig. 14.

Then, on the left of the intersection, with diameters below 0.2 µm, both tests have more volatiles than friction debris. On the right of the intersection, with diameters above 0.2 µm, friction tests are dominated by friction debris, while heating tests have more volatiles than friction debris. There should be a competitive mechanism of friction debris and volatiles, though not yet proven, that volatiles could be adsorbed by friction debris or split into smaller ones. If so, volatiles on the right of intersection in friction tests were adsorbed by friction debris, while in heating tests most volatiles remained due to much less friction debris. This is also in accordance with the high-temperature behaviour of airborne particles in Figs. 8 and 9. The airborne particles removed by the high-temperature version of ELPI + in friction tests were mostly with diameters below 0.3 µm which is very similar to the turning point of volatiles and friction debris. Perricone [11] discussed a turning point of 0.2 µm to divide the size distribution into semi-volatile part (below) and non-volatile part (above), with which the results of this study matched well. Many coarse particles were removed in

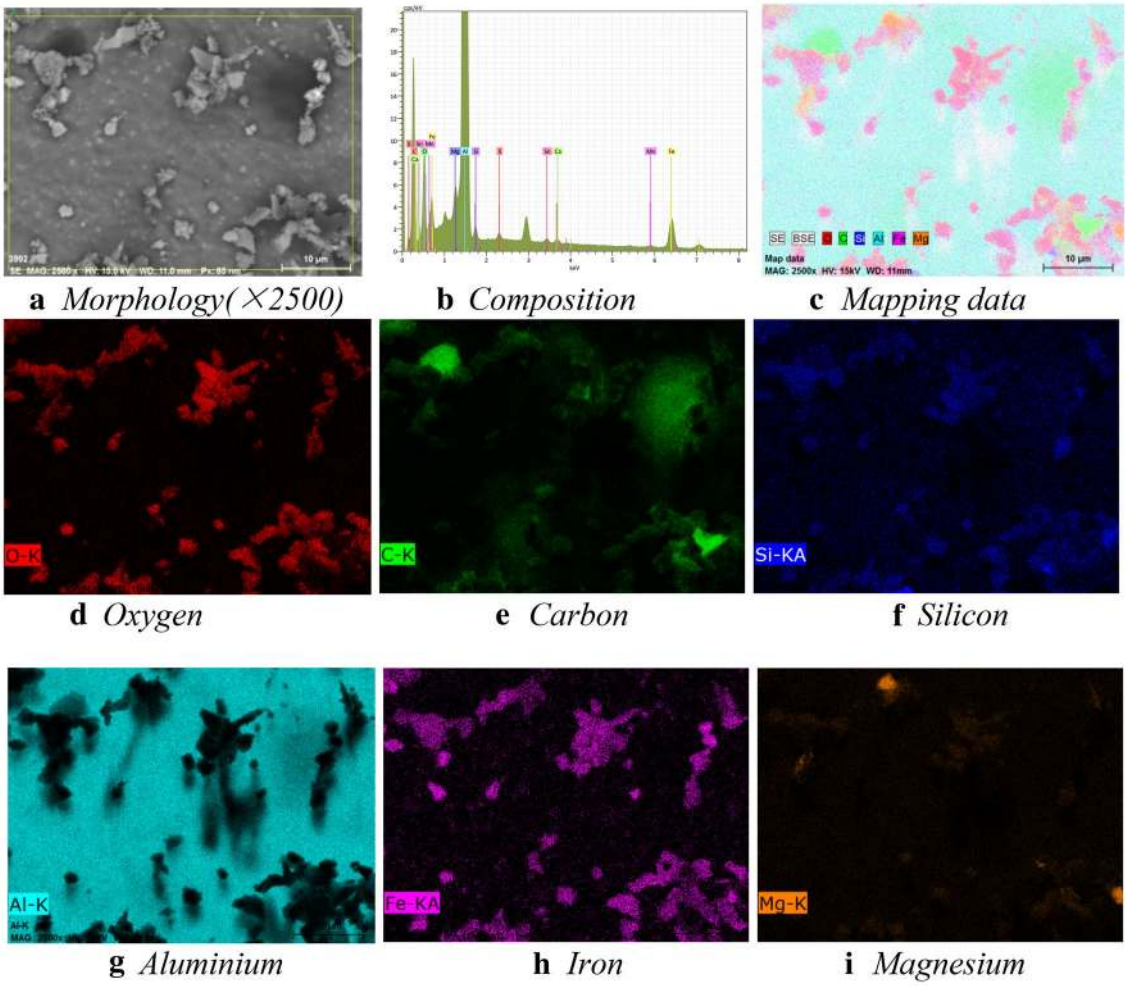

Fig. 13 Energy mapping of particles in channel 13 of Fric23

heating tests but not in friction tests, which could also be due to the fraction of volatiles in these channels.

Identification of temperature oriented non-friction airborne particles could be a support to scorching which is used in manufacturing of brake pads to reduce bedding-in time and initial fading. Since the test setup in this study is very similar to the scorching process, it provides another consideration to scorching parameters concerning brake emissions. Some further researches are meaningful to make clear the non-friction airborne particles at scorching temperature range.

4.2 Coarse Particles in Heating Tests

Coarse particles in heating tests were confirmed by both the particle number (Fig. 5) and the composition (Fig. 12). However, the origin of these coarse particles is still not clear as resuspension is another possible source. Although instruments indicated that the ambient particle number was zero before sharp increase, as shown in zone A of Fig. 15, it is not enough to make a conclusion since the coarse particles were low in number that might be beyond the resolution of the instruments.

An effective way is to observe the time history of the ELPI + raw current. Figure 15 demonstrates the time history of test Heat23_1 in terms of particle number and

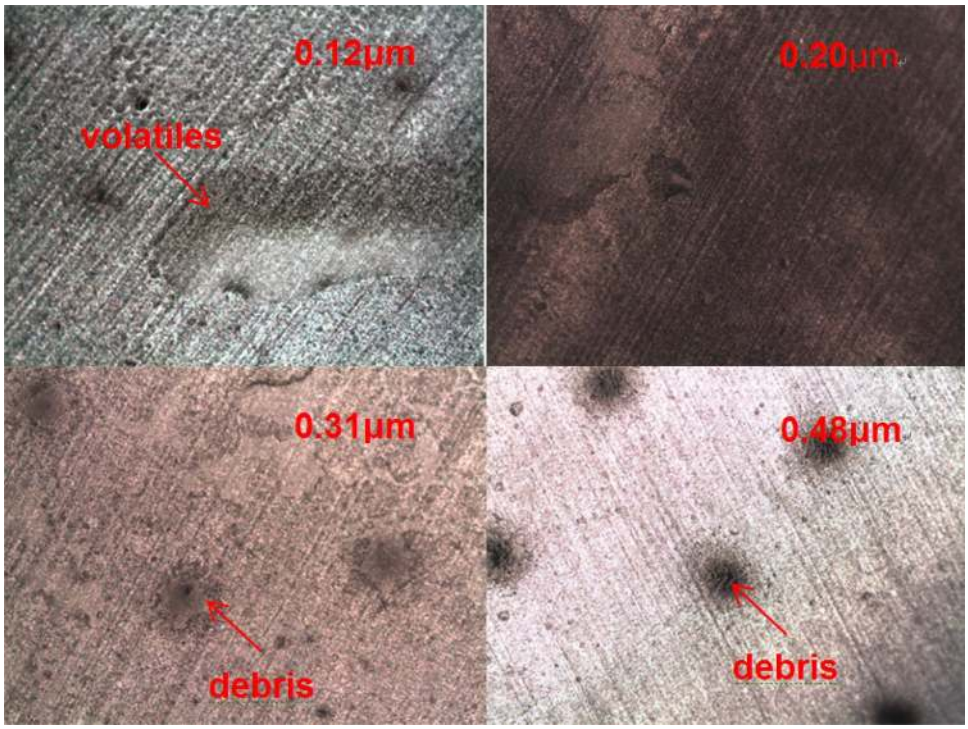

Fig. 14 Particles around 0.2 μm

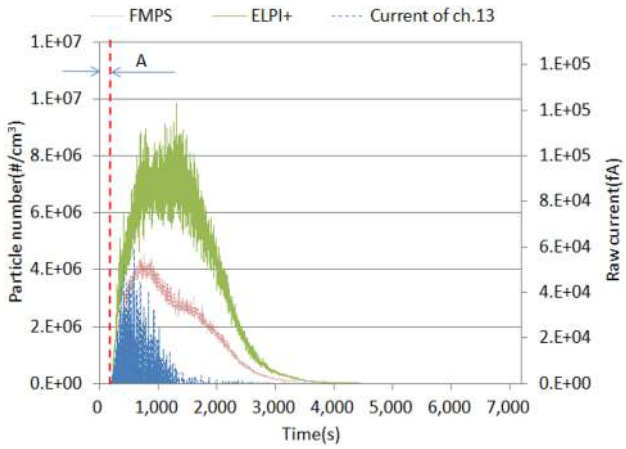

Fig. 15 Time history of Heat23_1

raw current of channel 13 (3 μm). It is clear that the raw current of channel 13 has a similar trend to the particle number concentration. This negates the possibility of a resuspension mechanism whose raw current should be decreasing from the very beginning of the test with the sealed chamber and constant airflow.

Ruling out resuspension, the most likely origin of coarse particles in heating tests is the friction pair. As for coarse particle generation in heating tests, a possible explanation could be the decoupling of the bonded friction materials from the surface of the pin due to high temperature. As temperature increases, some of the binders and fillers will degrade and the pin will expand. The friction materials on the surface of the pin will become airborne particles: some binders and fillers become volatiles and some decoupled reinforcing fibres and fillers become solid coarse particles. Volatiles in gas phase, according to Hinds [19], could further enhance the possibility of a solid coarse particle being airborne by surrounding it.

5 Conclusion

Airborne particles originated from the friction pair at elevated temperatures were studied by comparing stationary inductive heating and sliding friction tests. The high-temperature behaviour and the composition of non-friction airborne particles are also presented. The main conclusions of this paper include:

1. The heated friction pair can generate non-friction airborne particles without a sliding process.
2. Non-friction airborne particles can contribute about 5% in particle number in friction tests around 200 °C.
3. For airborne particles generated at around 200 °C of the friction pair, 30% is removed in heating tests and 90% are removed in friction tests by using a heated sampling line at 180 °C.
4. Ultrafine particles dominate the particle number in both heating and friction tests by fractions of 82% and 98%,

while the volume fractions are 1% and 19%, respectively. Composition analysis indicates a major fraction of volatiles in the ultrafine channels for both heating and friction tests.

Acknowledgements Open access funding provided by Royal Institute of Technology. This research receives funding from the project "ECO-PADS: Eliminating Copper from brake PADS and Recycling" funded by EIT Raw Materials. One of the authors gratefully acknowledges the Chinese Scholarship Council for its financial support.

References

1. Nosko, O., Olofsson, U.: Effective density of airborne wear particles from car brake materials. J Aerosol Sci **107**, 94–106 (2017). https://doi.org/10.1016/j.jaerosci.2017.02.014
2. Puisney, C., Oikonomou, K., Nowak, S., Chevillot, A., Casale, S., Baeza-Squiban, A., Berret, J.: Brake wear (nano)particle characterization and toxicity on airway epithelial cells in vitro. Environmental Science: Nano **5**(4), 1036–1044 (2018). https://doi.org/10.1039/C7EN00825B
3. Amato, F.: Non-exhaust emissions: an urban air quality problem for public health, impact and mitigation measures. Academic Press, London (2018)
4. ChihChung, L., ShuiJen, C., KuoLin, H., WenIng, H., Guo, P., Chang, C., WenYinn, L.: Characteristics of metals in nano/ultrafine/fine/coarse particles collected beside a heavily trafficked road. Environ Sci Technol **39**(21), 8113–8122 (2005). https://doi.org/10.1021/es048182a
5. Timmers, R.J.H.: Achten AJ (2016) Non-exhaust PM emissions from electric vehicles. Atmos Environ **134**, 10–17 (2016). https://doi.org/10.1016/j.atmosenv.2016.03.017
6. Wahlström, J., Olander, L., Olofsson, U.: A pin-on-disc study focusing on how different load levels affect the concentration and size distribution of airborne wear particles from the disc brake materials. Tribol Lett **46**(2), 195–204 (2012). https://doi.org/10.1007/s11249-012-9944-5
7. Wahlström, J., Matějka, V., Lyu, Y., Söderberg, A.: Contact pressure and sliding velocity maps of the friction, wear and emission from a low-metallic/cast-iron disc brake contact pair. Tribol Ind **39**(4), 460–470 (2017). https://doi.org/10.24874/ti.2017.39.04.05
8. Alemani, M., Wahlström, J., Olofsson, U.: On the influence of car brake system parameters on particulate matter emissions. Wear **396–397**, 67–74 (2018). https://doi.org/10.1016/j.wear.2017.11.011
9. Zum Hagen, F., Mathissen, M., Grabiec, T., Hennicke, T., Rettig, M., Grochowicz, J., Vogt, R., Benter, T.: Study of brake wear particle emissions: impact of braking and cruising conditions. Environ Sci Technol **53**, 5143–5150 (2019). https://doi.org/10.1021/acs.est.8b07142
10. Mathissen, M., Grochowicz, J., Schmidt, C., Vogt, R., Farwick Zum Hagen, F., Grabiec, T., Steven, H., Grigoratos, T.: A novel real-world braking cycle for studying brake wear particle emissions. Wear **414**(415), 219–226 (2018). https://doi.org/10.1016/j.wear.2018.07.020
11. Perricone, G., Matějka, V., Alemani, M., Wahlström, J., Olofsson, U.: A test stand study on the volatile emissions of a passenger car brake assembly. Atmosphere **10**(5), 263 (2019). https://doi.org/10.3390/atmos10050263
12. Plachá, D., Vaculík, M., Mikeska, M., Dutko, O., Peikertová, P., Kukutschová, J., Mamulová, K., Růžičková, J., Tomášek, V.: Filip P (2017) Release of volatile organic compounds by oxidative wear of automotive friction materials. Wear **376**(377), 705–716 (2017). https://doi.org/10.1016/j.wear.2016.12.016
13. Nosko, O., Olofsson, U.: Quantification of ultrafine airborne particulate matter generated by the wear of car brake materials. Wear **374–475**, 92–96 (2017). https://doi.org/10.1016/j.wear.2017.01.003
14. Milenkovic, P.D., Jovanovic, S.J., Jankovic, A.S., Milovanovic, M.D., Vitosevic, N.D., Djordjevic, M.V., Raicevic, M.M.: The influence of brake pads thermal conductivity on passenger car brake system efficiency. Thermal Sci **14**(Suppl S), S221–S230 (2010). https://doi.org/10.2298/TSCI100505016M
15. Wu, Y., Jin, H., Li, Y., Ji, Z.: Hou S (2014) Simulation of temperature distribution in disk brake considering a real brake pad wear. Tribol Lett **56**(2), 205–213 (2014). https://doi.org/10.1007/s11249-014-0400-6
16. Wahlström, J., Gventsadze, D., Olander, L., Kutelia, E., Gventsadze, L., Tsurtsumia, O., Olofsson, U.: A pin-on-disc investigation of novel nanoporous composite-based and conventional brake pad materials focussing on airborne wear particles. Tribol Int **44**(12), 1838–1843 (2011). https://doi.org/10.1016/j.triboint.2011.07.008
17. Olofsson, U., Olander, L., Jansson, A.: A study of airborne wear particles generated from a sliding contact. J Tribol **131**(4), 044503 (2009). https://doi.org/10.1115/1.3176990
18. Directive 2004/42/CE of the European Parliament and the Council: EUR-Lex. European Union Publications Office (2004) https://eur-lex.europa.eu/legal-content/EN/TXT/?uri=celex%3A32004L0042
19. Hinds, W.C.: Aerosol technology: properties, behaviour, and measurement of airborne particles. Wiley, New York (1999)
20. Nosko O, Vanhanen J, Olofsson U (2017) Emission of 1.3–10 nm airborne particles from brake materials. Aerosol Sci Technol 51(1):91–96. https://doi.org/10.1080/02786826.2016.1255713
21. Kukutschová, J., Moravec, P., Tomásek, V., Matejka, V., Smolík, J., Schwarz, J., Seidlerová, J., Safárová, K., Filip, P.: On airborne nano/micro-sized wear particles released from low-metallic automotive brakes. Environ Pollut **159**, 998–1006 (2017). https://doi.org/10.1016/j.envpol.2010.11.036